IEEE Access
Multidisciplinary ⋮ Rapid Review ⋮ Open Access Journal

Received 16 June 2024, accepted 19 July 2024, date of publication 23 July 2024, date of current version 20 August 2024.

Digital Object Identifier 10.1109/ACCESS.2024.3432691

RESEARCH ARTICLE

Using Deep Learning-Based Methods for Automated Segmentation of Soft Tissues From Shoulder Ultrasound Images

YING-CHUN LEE[1,2], CHIH-YANG LIN[1,3], (Senior Member, IEEE), CHIA-CHUN HSIAO[1,2], PU-CHUN MO[1], JIAQI GUO[1], AND YIH-KUEN JAN[1]

[1]Rehabilitation Engineering Laboratory, Department of Kinesiology and Community Health, University of Illinois at Urbana–Champaign, Urbana, IL 61820, USA
[2]Department of Electrical Engineering, Yuan Ze University, Taoyuan 320315, Taiwan
[3]Department of Mechanical Engineering, National Central University, Taoyuan 320317, Taiwan

Corresponding author: Yih-Kuen Jan (yjan@illinois.edu)

This work involved human subjects or animals in its research. Approval of all ethical and experimental procedures and protocols was granted by the University of Illinois at Urbana-Champaign under Application No. IRB #20405.

ABSTRACT Shoulder pain and injuries present significant challenges to researchers and clinicians for diagnosing underlying structural changes due to the complexity of the shoulder joint. Ultrasonography has been used for diagnosing shoulder impairment and can non-invasively assess structures and mechanical properties of the shoulder. However, the complexity of the shoulder structures often results in diagnostic difficulties and misdiagnosis. Although deep learning of artificial intelligence has been applied in various biomedical imaging, the adoption of deep learning techniques in the segmentation of musculoskeletal ultrasound images, especially the shoulder, is limited. This study addresses this gap by assessing the effectiveness of 3 deep learning models, U-Net, Mask R-CNN, and DeepLab V3+, for the segmentation of soft tissues from shoulder ultrasound images. We collected 721 images from the shoulder area of 17 healthy adults, including the anterior deltoid, medial deltoid, posterior deltoid, and supraspinatus. We employed a combination of three augmentation methods (elastic transform, horizontal flip, and shift scale rotate) to enhance the dataset. The mixed augmentation strategy resulted in U-Net outperforming Mask R-CNN and DeepLab V3+ with a mean Average Precision (mAP) of 78-81%, a mean Intersection over Union (mIoU) of 81-87%, and Recall and Precision values between 91-94% and 87-91%, respectively. The effective use of deep learning methods could assist clinicians on assessing shoulder structures from ultrasound images.

INDEX TERMS Artificial intelligence, computer assisted diagnosis, muscle, and ultrasonography.

I. INTRODUCTION

Improper and over use of shoulder muscles can lead to shoulder pain and injury [1]. Athletes who repetitively strain their shoulders may develop conditions, such as shoulder impingement syndrome, characterized by persistent shoulder pain and weakness [2], [3]. These shoulder problems can significantly impact their activities of daily living, leading individuals to seek medical attention to manage this musculoskeletal impairment [4]. Due to the complex structure of the shoulder joint, the manual examination by the clinician is usually not able to accurately identify the underlying impairment for shoulder pain. In recent years, the use of ultrasound imaging has been becoming a popular tool to accurately identify the underlying cause of pain [4], [5]. Through real-time diagnosis of the musculoskeletal structure of the shoulder joint, clinicians can examine the specific location and structure of the soft tissue of the shoulder for identifying pathological changes. Clinically, accurately locating the soft tissue injury from musculoskeletal ultrasound images can be challenging

The associate editor coordinating the review of this manuscript and approving it for publication was Tao Huang.

because of the complex shoulder joint consisting of bones, muscles, tendons, and nerves.

To identify the components (eg. muscle and tendon) from the musculoskeletal ultrasound images, the segmentation of each component is paramount, serving as a crucial step for injury diagnosis and healing monitoring. Bonaldi et al. pointed out the importance of medical image segmentation, particularly in analyzing ultrasound images of musculoskeletal structures [6]. However, most of the segmentation methods have been developed for computed tomography (CT) and magnetic resonance imaging (MRI), and only a few studies focused on ultrasound images. In the MRI images of the upper limb, research studies have explored region-based methods, deformable models, and deep-learning approaches [7]. Investigations in the lower limb and trunk have used manual, semi-automated, and fully automated methods, contributing to our understanding of muscle segmentation techniques, their accuracy, and potential applications in clinical settings. Building on this foundation, the application of computer-assisted diagnosis with ultrasound in the field of sports medicine has revolutionized the precise segmentation of muscles and tendons. Liu et al. introduced an innovative segmentation algorithm for the identification of carcinoma area from the ultrasound images, employing deep feature fusion to segment muscles and tendons with impressive accuracy [8]. Their research underscores the indispensable role of ultrasound image segmentation, particularly in the examination of muscles and tendons from ultrasound images. Lumsden et al. incorporated the upper limb and shoulder assessment for improving the segmentation of structures from the ultrasound image [9]. These studies demonstrate the important role of ultrasound image segmentation in medical practice, highlighting its potential to improve injury assessment and rehabilitation.

Among medical imaging modalities, ultrasound has emerged as a particularly valuable tool, especially in musculoskeletal imaging, due to its unique advantages. Nobel and Boukerroui highlighted the value of ultrasound imaging in the musculoskeletal system due to its non-invasive nature, real-time imaging capabilities, and the ability to provide high-resolution images of subcutaneous tissue and structures [10]. It is frequently employed for diagnostic purposes, such as identifying musculoskeletal injuries, joint effusions, and tendon abnormalities. Ultrasound imaging holds several advantages over other imaging modalities, such as CT and MRI. First, ultrasound is non-invasive and does not employ ionizing radiation, unlike CT scans, making it safer for repeated use and particularly suitable for special populations, like pregnant women and children. Second, ultrasound provides real-time imaging, a feature that allows clinicians to observe the movement of internal organs and blood flow in vessels. Third, ultrasound is a cost-effective option that is generally less expensive than their CT and MRI counterparts [11]. Additionally, the portability of ultrasound machines is a significant advantage that can be easily transported and used at the patient's bedside, unlike large and stationary CT and MRI machines. In clinical practice, ultrasound remains the most widely used imaging modality. While ultrasound imaging offers numerous advantages, its limitations include lower resolution, image blur, noise, low contrast, and significant variations between images. Moreover, in clinical settings, medical images are typically interpreted by humans, and broad variations in pathology can place a significant burden on clinical specialists and physicians. Given these challenges, segmentation of various structures (eg. muscles, tendons, and fat) becomes a crucial task in musculoskeletal ultrasound. Additionally, previous studies on ultrasound image segmentation, such as the work by Zhao et al. [12], have identified several limitations. These include susceptibility to artifacts and the influence of echo, shadow, and reflection, which can degrade the quality of the acquired images. The study further emphasizes the need for substantial computational resources, including large memory capacity and intensive calculations. These challenges often hinder the achievement of consistent and reliable segmentation, especially in anatomically complex regions like the shoulder joint. In light of these limitations, Deep Learning (DL) techniques offer a promising avenue for improvement in musculoskeletal ultrasound diagnosis. DL models have the potential to enhance image resolution and reduce noise, thereby facilitating more accurate and reliable clinical interpretation and diagnosis. [13] DL could aid in the clinical diagnosis and treatment of conditions like rotator cuff tears and tendinitis by providing valuable information for treatment planning and assessing the effectiveness of interventions. Segmentation enables biomechanical analysis, assisting in understanding muscle activation patterns and mechanics during shoulder movements. Tokuda et al. explored muscle activation patterns during reach-to-grasp movement, focusing on the shoulder muscles' role in different phases of reaching movements [14]. Eriksson Crommert et al. investigated trunk muscle activation patterns during rapid bilateral shoulder flexions, emphasizing the need to standardize arm movements [15]. These studies highlight the importance of segmentation of various muscles in biomechanical analysis, particularly in the context of shoulder movements. In addition, segmentation of the structures from ultrasound images helps surgical planning by guiding surgeons in visualizing affected structures and achieving optimal outcomes. In conclusion, precise segmentation of musculoskeletal ultrasound images is invaluable for image-guided interventions, enhancing accuracy and safety during procedures like injections.

However, despite these advantages of using deep learning for ultrasound diagnosis, many clinicians have yet to adopt deep learning-based segmentation methods for diagnosis, continuing to rely on conventional segmentation methods. Traditional techniques often require extensive prior knowledge and numerous attempts at arranging and combining various elements, and they can be easily influenced by factors

such as field of view, inclination, illumination, and noise [16]. In stark contrast, the rapid advancement of deep learning and artificial intelligence in medical imaging has shown remarkable promise, far surpassing conventional methods [17], [18], [19], [20], [21]. Brehar et al. compared deep-learning and conventional machine learning methods for the automatic recognition of hepatocellular carcinoma areas from ultrasound images and found the superior performance of deep-learning approaches compared to conventional machine learning methods [22]. Deep learning offers the potential for accurately diagnosing, precisely segmenting, classifying, and predicting various diseases through quick and accurate processing of ultrasound images. Various deep learning models have been demonstrated for producing significant attention and demonstrating great promise in improving the accuracy and efficiency of disease diagnosis and classification by authors such as Ronneberger et al. [23], who introduced the U-Net architecture, He et al. [24], who developed Mask R-CNN, and Chen et al. [25], who proposed DeepLab V3+. Despite these advancements, to our knowledge, deep learning-based research has yet to be conducted specifically on segmenting B-mode ultrasound images of the shoulder joint. The contrast between traditional methods and the capabilities of deep learning techniques emphasizes the urgent need for further exploration and adoption of these advanced models in medical practice, particularly in the context of ultrasound imaging.

While data augmentation techniques have been extensively studied in various medical imaging modalities and anatomical structures, their application to ultrasound imaging of the shoulder joint is less explored. Nonetheless, a comprehensive survey [26] provides strong evidence for the generalizability of data augmentation methods such as rotation, flipping, and scaling across different types of medical imaging (Shorten and Khoshgoftaar 2019. These techniques have proven effective in enhancing model performance and are widely applicable, including in medical image analysis. Therefore, leveraging these established methods could offer a viable strategy for improving the accuracy and robustness of deep learning-based segmentation models for the shoulder joint, without the need for developing entirely new augmentation techniques.

In this study, the deep learning-based segmentation methods were compared to segment the soft tissue of the shoulder ultrasound images, including the subcutaneous tissue, muscles, and tendons. Specifically, U-Net [23], Mask R-CNN [24], and DeepLab V3+ [25] have been used to segment shoulder structure of the ultrasound image. Furthermore, using the outcomes from our segmentation model, such as U-Net, we explored whether specific regions from the ultrasound images could be cropped out for further quantification analysis. We then computed the mean error and standard deviation for both the labeled muscle areas in the ground truth and the regions segmented by our models. This quantitative approach serves as a robust metric for assessing the model's performance. The mean pixel value and its standard deviation are commonly used in medical imaging to provide insights into tissue characteristics, thereby ensuring diagnostic accuracy and reliability [27]. The application of machine learning in segmenting musculoskeletal ultrasound images, particularly of the shoulder joint, still needs to be explored. The primary objective of this study was to evaluate the comparative effectiveness of three deep learning techniques (U-Net, Mask R-CNN, and DeepLab V3+) in segmenting soft tissues from shoulder ultrasound images. The secondary objective was to assess the effectiveness of three augmentation methods (elastic transform, horizontal flip, and shift scale rotate) to enhance the dataset of ultrasound images.

II. MATERIAL AND METHODS

A. ULTRASOUND IMAGES

The study involved capturing ultrasound images from 13 distinct locations (planes) on the shoulder to evaluate the soft tissue, including the muscles, tendons and joint space. Musculoskeletal ultrasound images, a unique type of biomedical image, present their own set of challenges for segmentation using deep learning algorithms. Unlike other medical images, musculoskeletal ultrasound images have specific features that make segmentation more difficult, especially the use of a limited number of 2D ultrasound images to characterize a 3D structure [28]. One of the main challenges is the regular movement of muscles, which can result in noise in the images. This noise can affect the effectiveness of the deep learning results. Additionally, the area-specific nature of skeletal muscle classification requires a cropping strategy, which adds another layer of complexity to the segmentation process [29]. Despite these challenges, deep learning algorithms hold great promise for improving the diagnosis and treatment of musculoskeletal conditions. An elastography ultrasound device (ProSound A7; Hitachi Healthcare Americas, Twinsburg, OH) [30] was used to measure the shoulder muscle (long head of biceps brachii muscle and tendon [31], supraspinatus muscle and tendon [32], infraspinatus muscle, deltoid (anterior and medial) muscles and biceps muscle) in healthy adults. The ultrasound probe operates within a frequency range of 17–21 MHz (UST-5412; Hitachi Healthcare Americas), with a selected operational frequency of 17 MHz for this study. This frequency was chosen because of its optimal balance between penetration depth and image resolution, making it ideal for our specific application in medical imaging [33]. The probe utilizes a phased array transducer, which allows for a wide field of view and high-resolution imaging capabilities. Additionally, we have configured the probe to function at an 8 MHz frequency, with a depth setting of 7.5R and a gain level of 70. Our training and validation data consisted of 721 images from 17 healthy adults. In Figure 1, we evaluated five areas of each participant's shoulder structure, specifically (a) anterior deltoid, (b) medial deltoid, (c) posterior deltoid, (d) supraspinatus, and (e) horizontal supraspinatus), along with B-mode images of the supraspinatus. For the anterior deltoid, medial deltoid, posterior deltoid, and

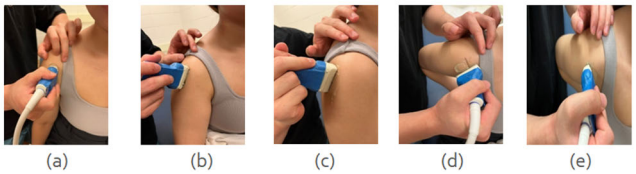

FIGURE 1. From left to right, the pictures show five areas of the shoulder: (a) Anterior Deltoid, (b) Median Deltoid, (c) Posterior Deltoid, (d) Supraspinatus, and (e) Horizontal Supraspinatus.

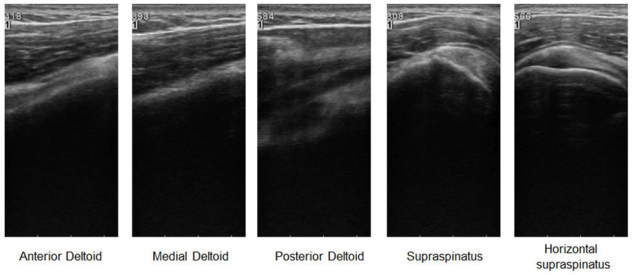

FIGURE 2. B-mode ultrasound images correspond to the five distinct areas of the shoulder structure of Figure 1.

supraspinatus, the subcutaneous tissue, muscle, and tendon were marked into three portions because the muscles intended for recording would overlap, as shown in Figure 1. Each area, except for the horizontal supraspinatus, was measured three to five times to ensure data completeness. The horizontal supraspinatus was only measured once due to the limited space available. Additionally, for each position, we collected data three to five times. Figure 2 illustrates the corresponding locations of ultrasound images in our study.

B. IMAGE LABELING

We labeled our data with muscles, tendons, and subcutaneous tissue through LabelMe. LabelMe is a graphical image annotation tool in Python that uses Qt for its interface [34]. In Figure 3, the B-mode images on the right-hand side of panels (a), (d), and (e) show that the top layers typically consist of subcutaneous tissues and muscles. The lower layers are generally composed of muscles and tendons, with muscle borders appearing darker than tendons. A brighter border at the bottom of these images, extending beneath the black area, signifies bone. In some positions, such as in panels (b) and (c), tendons are not visible. Our study focuses primarily on subcutaneous tissue, so we opted not to label the bone regions. Occasionally, the presence of human fat can make the boundary between subcutaneous tissue and muscle less distinct, adding complexity to the labeling task [35]. Figure 3 displays the images we successfully labeled through manual annotation by the authors with clinical expertise on using ultrasound [30], [33], while Figure 3 features the images that posed challenges for labeling. As for the anterior deltoid, medial deltoid, posterior deltoid, and supraspinatus, we marked the subcutaneous tissue, muscle, and tendon into

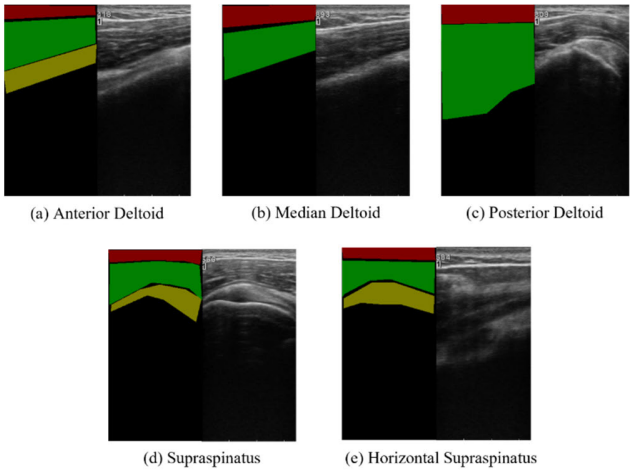

FIGURE 3. Each picture demonstrates the labeled picture (left side) and the original ultrasound image (right side). Red stands for the subcutaneous tissue, green is the muscle, and yellow is the tendon.

three portions for each position and then took three images on each portion.

C. SEGMENTATION

To optimize the learning process of our model, we employed a two-fold data partitioning strategy: Intra-subject and Inter-subject. This approach was inspired by the work of Saha and Baumert [36], who emphasized the importance of considering both intra- and inter-subject variability in data partitioning. Our methodology was further informed by the study of Nguyen et al. [37], which examined the influence of data splitting ratios on machine learning model performance. In the Intra-subject form, data from each participant were randomly mixed, ensuring that both the training and validation datasets included images from all participants, albeit without any overlap. For the Inter-subject form, we allocated the data from two randomly selected participants for validation, while the data from the remaining 15 participants constituted the training set. Although the study by Nguyen et al. utilized an 80/20 training-to-testing ratio, we opted for a 90/10 split for our training and validation sets [37]. This deviation was motivated by our collection of a separate, individual test set. We hypothesized that a larger training set would enhance the model's accuracy, particularly given that our total dataset of 721 training and validation images is relatively small for deep learning applications. This hypothesis is supported by the research of An et al. [38], which emphasizes the challenges and potential solutions when applying deep learning models to small medical image datasets. Our two-fold partitioning strategy aims to account for both intra- and inter-subject variability, thereby enhancing the model's generalizability and robustness.

1) U-NET

U-Net is a convolutional network architecture for fast and precise segmentation of images and has been widely adopted

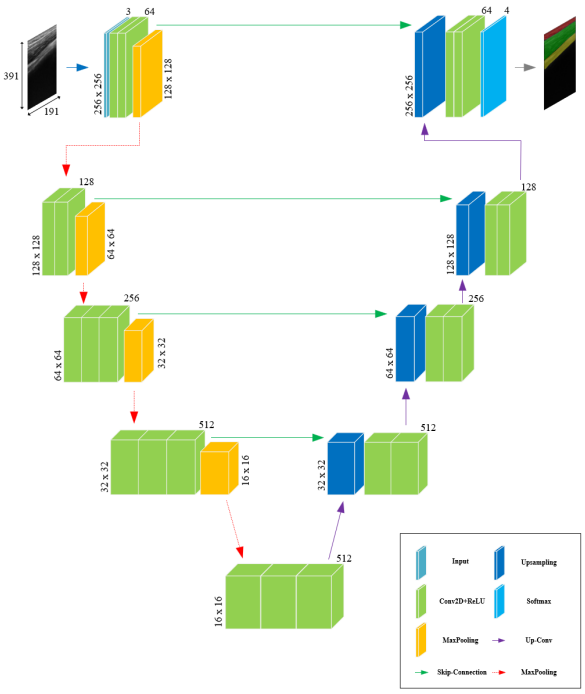

FIGURE 4. Structure of the U-Net.

in biomedical image segmentation due to its effectiveness on smaller datasets and the ability to capture detailed features [23]. The architecture also includes skip connections, which help in preserving intricate details that might be lost during the encoding process. Furthermore, U-Net's ability to perform multi-scale feature extraction allows it to capture both global and local image information, making it particularly effective for ultrasound image segmentation. Meanwhile, It has been successfully applied in various biomedical applications, including dental X-ray and EM image segmentation [39]. The structure of U-Net is shown in Figure 4.

2) MASK R-CNN

Mask R-CNN is an extension of Faster R-CNN and is another deep learning model, for instance, segmentation tasks. It extends Faster R-CNN by adding a branch for predicting an object mask in parallel with the existing branch for bounding box recognition [24]. This additional branch allows Mask R-CNN to handle complex structures, tissues, and organs in medical images, making it particularly useful for ultrasound image segmentation. Furthermore, Mask R-CNN reuses low-level feature information, which can be beneficial for segmenting specific organs [40]. The structure of Mask R-CNN is shown in Figure 5.

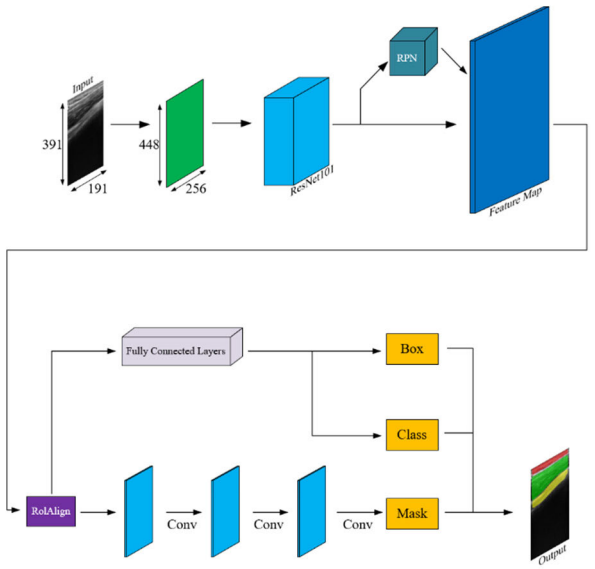

FIGURE 5. Structure of the Mask R-CNN.

3) DEEPLAB V3+

DeepLab V3+ is an encoder-decoder structure for semantic image segmentation. It combines the advantages of both the spatial pyramid pooling module and encoder-decoder structure, thereby enabling effective segmentation of objects at multiple scales. This architecture is particularly beneficial for ultrasound image segmentation as it can handle complex structures and tissues in medical images. Furthermore, DeepLab V3+ reuses low-level feature infor-

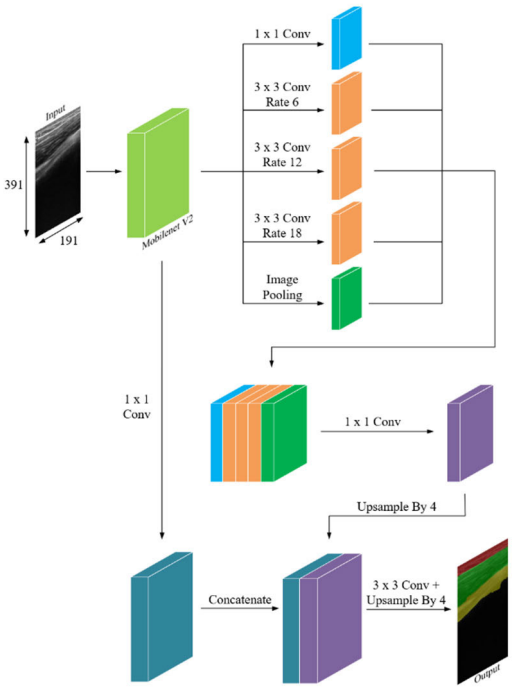

FIGURE 6. Structure of the DeepLab V3+.

mation, which can be beneficial for segmenting specific organs [41]. The structure of DeepLab V3+ is shown in Figure 6.

D. MIXED DATASET

We implemented a Mixed Dataset that combined three augmentation methods: horizontal flip, elastic transform, and shift scale rotation [42]. Specifically, we applied these augmentations with probabilities of 20%, 20%, and 10%, respectively, using the Sometimes function. This means that each image in the dataset had a 20% chance of being horizontally flipped, a 20% chance of undergoing elastic transformation, and a 10% chance of being shifted, scaled, or rotated. The remaining 50% of the dataset consisted of the original, un-augmented images. This approach aimed to achieve better segmentation results by introducing variability into the dataset, compared to using a single augmentation method.

E. AUGMENTATION METHODS

In the augmentation settings for shift-scale-rotate, we set the shift to ± 0.0625, the scale to ± 0.1, and the rotation to ± 15 degrees. For the elastic transform function, we set alpha to 120 and sigma to 6. After completing all parameter settings, we train U-Net and DeepLab V3+ in 300 epochs and Mask R-CNN in 150 epochs, with the first 100 epochs dedicated explicitly to the head layer of Mask R-CNN. This approach prevents overfitting by ensuring the model learns task-specific features before more abstract ones and enhances training efficiency. The models were trained on 32, 8, and 32 batch sizes corresponding to U-Net, Mask R-CNN, and DeepLab V3+, respectively. All mentioned models have been implemented using TensorFlow 2.10 (Unet & DeepLab V3+) and 2.5 (Mask R-CNN) with Cuda 11.8 in a computer with an RTX 4090. The U-Net and DeepLab V3+ code used in this study is based on the GitHub repository by bubbliiiing [43], [44]; for Mask R-CNN we edited the implementation available in the repository by zouyuelin [45].

F. APPLICATIONS

We obtained both the B-mode image and its corresponding elastic image from the raw image data. After completing the labeling of the ultrasound image, we mapped the labeled area on the elastic image and divided it into three distinct parts: subcutaneous tissue, muscle, and tendon. We then calculated the mean of the non-zero pixels within these areas. Additionally, we computed the standard deviation for these values. Figure 7 illustrates the specific regions within the elastic image that were chosen for segmentation.

III. RESULTS

Table 1 offers a comprehensive assessment of our model's performance, utilizing key metrics such as mAP (Mean Average Precision), Precision, Recall, and mIoU (mean Intersection over Union). According to the data, the U-Net model emerges as the most fitting option for our requirements.

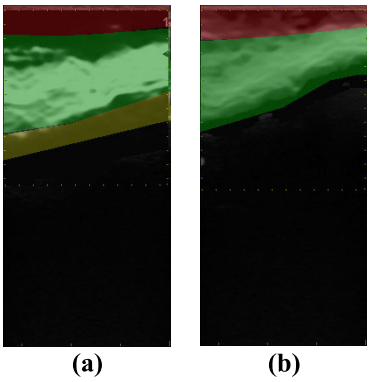

FIGURE 7. Mapping Labeled Regions onto the Elastic Image. (a) Anterior section of the shoulder with regions labeled in descending order: subcutaneous tissue, muscle, and tendon. (b) Median section of the shoulder labeled from top to bottom as subcutaneous tissue and muscle.

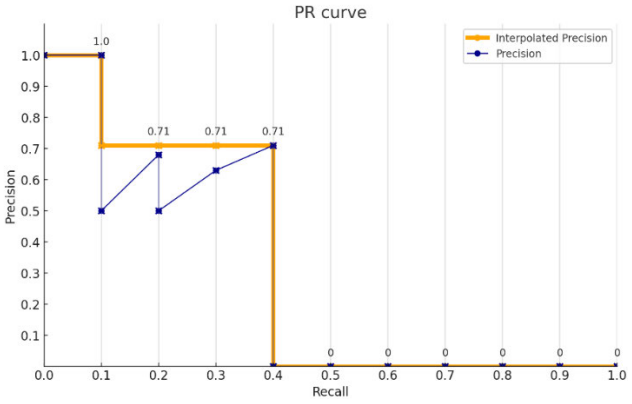

FIGURE 8. The standard precision-recall curve of mAP 11 Interpolated.

However, all three models—U-Net, DeepLab V3+, and Mask R-CNN—occasionally mislabel atypical positions.

To rectify this issue, we intend to incorporate data augmentation. This strategy will enable our model to discern more specific shoulder features and mitigate overfitting. Table 1 illustrates the finalized model, encapsulating our ultimate results. The mAP calculation was conducted based on the VOC2007 11-point interpolated average. VOC2007, or Visual Object Classes Challenge 2007, is a standard benchmark for evaluating object detection algorithms. The 11-point interpolated average refers to the method of calculating the AP (average precision) by interpolating the precision-recall curve at 11 equally spaced recall levels $[0, 0.1, \ldots, 1]$. Figure 8 depicts a standard precision-recall curve. The blue dots represent the original precision-recall points, showing a zig-zag pattern due to variability in the model's predictions at different recall levels. Beyond a recall of 0.5, all precision values drop to zero, indicating a large number of false positives. Despite these variations, the interpolated precision, represented by the purple line, provides a robust measure of the model's performance by considering the maximum precision value from each recall level onward.

As delineated in Table 1, the Precision and Recall for the U-Net model were 0.91 ± 0.02 and 0.94 ± 0.03 for the training set, 0.80 ± 0.09 and 0.93 ± 0.02 for the validation

TABLE 1. The mAP, precision, recall and mIoU results including intra- and inter-subject.

All		Intra-subject				Inter-subject			
		mAP	Precision	Recall	mIoU	mAP	Precision	Recall	mIoU
U-Net	Train	0.815	**0.917**	0.937	0.867	0.813	**0.915**	0.943	0.870
	Val	0.809	**0.911**	0.932	0.857	0.795	**0.896**	0.928	0.842
	Test	**0.785**	**0.883**	**0.913**	**0.816**	**0.781**	**0.878**	**0.917**	**0.815**
Mask R-CNN	Train	**0.999**	0.777	0.611	**0.941**	**0.999**	0.777	0.611	**0.958**
	Val	**0.959**	0.767	0.600	**0.912**	**0.910**	0.767	0.604	**0.885**
	Test	0.718	0.703	0.565	0.795	0.761	0.703	0.561	0.756
DeepLab V3+	Train	0.804	0.885	**0.946**	0.841	0.790	0.888	**0.944**	0.846
	Val	0.806	0.887	**0.948**	0.847	0.813	0.894	**0.953**	0.858
	Test	0.745	0.860	0.912	0.797	0.770	0.867	0.905	0.797

* The bold font indicates the best performance of a test.

TABLE 2. The efficiency results include intra- and inter-subject.

All-Efficiency	Intra-subject	Inter-subject
U-Net	**2376s**	**2378s**
Mask R-CNN	3530s	4025s
DeepLab V3+	7411s	7386s

* Bold font indicates the best performance of the test.

TABLE 3. The mean error and standard deviation results.

		Mean error	Standard Deviation
Ground Truth vs. U-Net	Subcutaneous Tissue	0.7256106	0.4915723
	Muscle	1.9154454	1.7933404
	Tendon	0.9074322	0.9817266
Ground Truth vs. Mask R-CNN	Subcutaneous Tissue	3.0711954	1.8240170
	Muscle	1.5148649	1.5153958
	Tendon	1.1889035	1.2144774
Ground Truth vs. DeepLab V3+	Subcutaneous Tissue	0.6856416	0.3871392
	Muscle	2.2739612	2.0922081
	Tendon	0.7104078	0.7059169

set, and 0.88 ± 0.03 and 0.91 ± 0.01 for the test set. For the DeepLab V3+ model, the corresponding values were 0.88 ± 0.01 and 0.94 ± 0.01 for the training set, 0.88 ± 0.01 and 0.95 ± 0.03 for the validation set, and 0.86 ± 0.01 and 0.91 ± 0.01 for the test set. Lastly, the Mask R-CNN model yielded 0.77 ± 0.01 and 0.61 ± 0.01 for the training set, 0.76 ± 0.01 and 0.60 ± 0.01 for the validation set, and 0.70 ± 0.01 and 0.56 ± 0.01 for the test set.

Table 2 illustrates the training time efficiency of each model, measured in seconds, for both Intra and Inter datasets. For the U-Net model, the training time was 2376 seconds for the Intra dataset and 2378 seconds for the Inter dataset. DeepLab V3+ took 7411 seconds for the Intra dataset and 7386 seconds for the Inter dataset, reflecting its computational complexity. Mask R-CNN recorded training times of 3164 seconds for the Intra dataset and 3276 seconds for the Inter dataset. These timings provide a nuanced insight into the computational efficiency of the models, reflecting the specific demands of different datasets and the inherent trade-offs between accuracy and computational cost [46]. The entire process was calculated from the initiation of the first code to the completion of the training stage, aligned with best practices in reproducible research [47], and offering a comprehensive view of the time efficiency for each model.

Table 3 presents the mean pixel values and the standard deviations of the delta values, comparing the ground truth with predictions from each of the models: U-Net, Mask R-CNN, and DeepLab V3+. For subcutaneous tissue, U-Net and DeepLab V3+ yield average results within the range of 0.6 to 0.7, while Mask R-CNN lags behind with a value of approximately 3. In muscle areas, the models register values between 1.5 and 2.2, and between 0.7 and 1.1 across all models. As for the standard deviation in subcutaneous tissue, U-Net and DeepLab V3+ perform within a range of 0.3 to 0.5, while Mask R-CNN shows a higher deviation of about 1.8. In both muscle and tendon areas, the standard deviations

TABLE 4. The IoU scores for each class include intra- and inter-subject.

IoU Score		Intra-subject	Inter-subject
U-Net	Subcutaneous Tissue	0.84	0.85
	Muscle	**0.81**	**0.80**
	Tendon	0.71	0.70
Mask R-CNN	Subcutaneous Tissue	**0.89**	**0.88**
	Muscle	0.80	0.79
	Tendon	**0.79**	**0.78**
DeepLab V3+	Subcutaneous Tissue	0.84	0.82
	Muscle	0.77	0.78
	Tendon	0.67	0.68

* Bold font indicates the best performance of the test.

vary from 1.5 to 2.1 and 0.7 to 1.2, respectively. Figure 9, on the other hand, displays the results for the Ground-Truth and the three models. The ground true images are A, E, I and M, U-Net images are B, F, J and N, Mask R-CNN images are C, G, K, and O, and DeepLab V3+ images are D, H, L, and P.

Table 4 presents the IoU scores for three anatomical areas—subcutaneous tissue, muscle, and tendon—across three deep learning models: U-Net, Mask R-CNN, and DeepLab V3+. The results indicate that subcutaneous tissue consistently achieved the highest IoU scores, ranging from 0.82 to 0.89, across all models. Muscle segmentation also yielded strong performance, with IoU scores ranging from 0.77 to 0.81. In contrast, tendon segmentation presented a more challenging task, as evidenced by its lower IoU scores, which ranged from 0.67 to 0.79. Notably, the differences in IoU scores between the Intra-subject and Inter-subject data partitions were minimal, suggesting that both partitioning strategies yielded comparable performance. This observation will be further discussed in the context of the challenges associated with tendon segmentation.

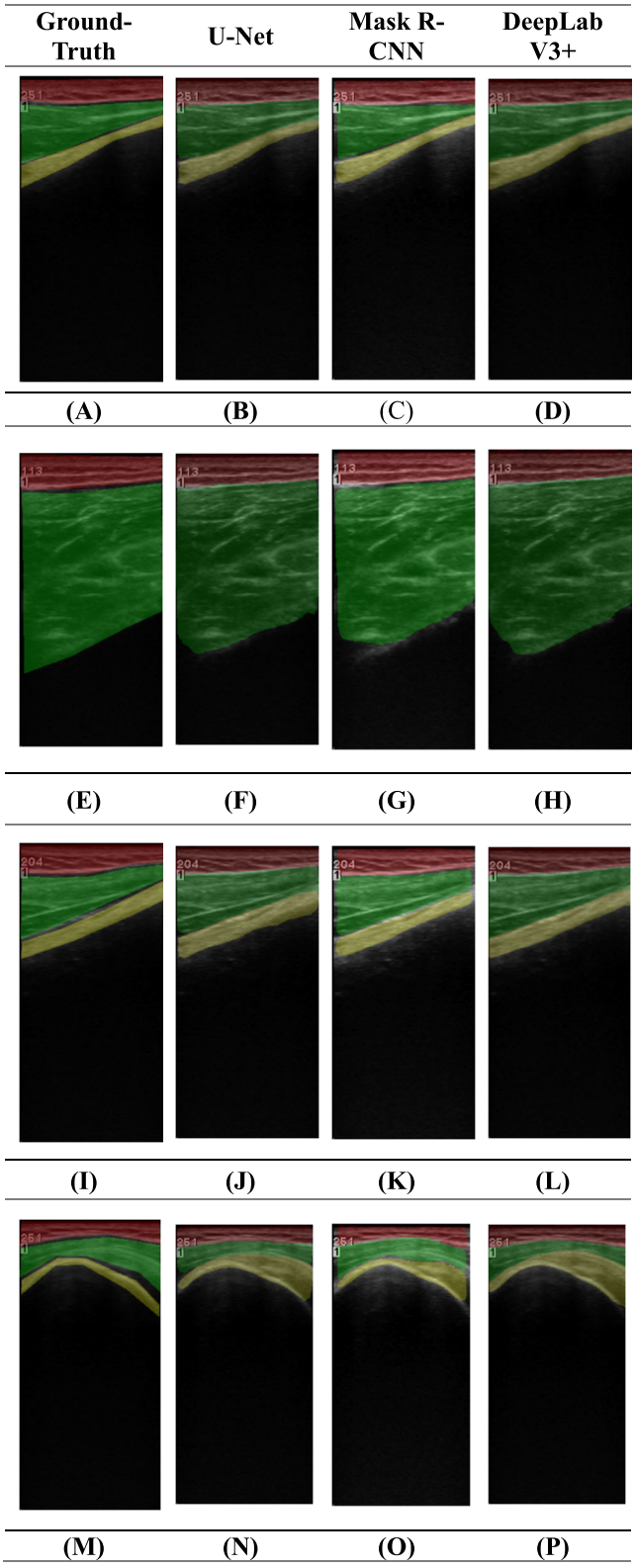

FIGURE 9. Comparison of the ground truth and predictions made by our model.

IV. DISCUSSIONS

A. COMPARATIVE ANALYSIS OF FINDINGS

In this study, we conducted a comparative analysis of three distinct deep learning models—U-Net, Mask R-CNN, and DeepLab V3+—in the medical imaging domain. This marks a significant step in evaluating these specific models for medical applications, particularly for the segmentation of shoulder muscles from ultrasound images. We noted the work of Lee et al. [48] and Wang et al. [49], which used different methodologies for diagnosing rotator cuff tears and segmenting supraspinatus from ultrasound images, respectively. Our study broadens the perspective by comparing the performance of these well-established models, providing insights into their strengths and weaknesses in ultrasound image segmentation. The results underscore the potential of

deep learning in aiding accurate diagnoses and streamlining workflow in medical practice, especially in the context of shoulder muscle segmentation. The disparities in performance metrics among the models emphasize the importance of model selection and fine-tuning, tailored to the dataset's unique characteristics. These insights, along with the work of Lee et al. [48] and Wang et al. [49], contribute to the ongoing development of deep learning techniques for ultrasound image analysis.

Following our comparative analysis, a consistent trend emerged across all models, muscle segmentation consistently achieved higher accuracy than tendon segmentation, as evidenced by the IoU scores presented in Table 4. This observation is supported by the findings of Kim et al. [50], which highlighted the inherent challenges of tendon segmentation due to ambiguous boundaries between tendons and muscles. Delving deeper into traditional imaging techniques, the study by Edmunds et al. provides valuable insights [51]. Their research emphasized the use of QCT (Quantitative Computed Tomography) and advanced image analysis tools to characterize muscles in 2D and 3D, underscoring the intrinsic differences between muscle and tendon. Such traditional imaging techniques, combined with our deep learning findings from Table 4, suggest that while models like U-Net are good at handling muscle tissue complexity, tendons present challenges that need further exploration and model fine-tuning.

B. COMPARATIVE ANALYSIS OF DEEP LEARNING MODELS

In our study, we evaluated three models: U-Net, DeepLab V3+, and Mask R-CNN. U-Net emerged as the superior model in terms of both accuracy and computational efficiency. This can be attributed to its symmetric encoder-decoder structure and the use of skip connections [23], which excel in precise localization of features, a crucial aspect in medical imaging tasks. In a study [52] focused on extracting water bodies from GaoFen-1 remote sensing images demonstrated U-Net's ability to extract detailed information, albeit with occasional confusion with objects having similar spectral characteristics. However, it may occasionally confuse objects with similar spectral characteristics. DeepLab V3+, while robust for general segmentation tasks due to its complex architecture and the integration of Trous separable convolution in both the ASPP (Atrous Spatial Pyramid Pooling) [25] and decoder modules, could risk overfitting when applied to limited datasets. It also showed certain limitations, such as missing parts of rivers and lakes and not effectively removing building shadows, suggesting potential overfitting. Mask R-CNN, despite its versatility with its mask prediction phase and the use of an RPN (Region Proposal Network) [24] for object classification and mask prediction, introduces computational challenges and potential error sources, especially when handling limited datasets. This could render it less apt for real-time applications and could hinder its efficacy in niche tasks. Despite these, DeepLab V3+ exhibited marked superiority in accuracy over Mask R-CNN, thanks to its specialized design that facilitates robust multi-scale feature extraction. However, U-Net's superior performance underscores the importance of considering structural differences and domain-specific requirements when selecting and applying these models. Our study aims to bridge the gap in the literature comparing these models in the realm of medical imaging and serve as a foundational reference.

C. OVERALL FINDINGS

In the evolving landscape of medical imaging, AI (Artificial Intelligence) models have shown considerable promise in enhancing the precision of anatomical segmentation. While our primary focus is not on elasticity imaging itself, the clinical relevance of such imaging techniques serves as a compelling example of how our models could be applied in real-world settings. Taljanovic et al. highlighted the use of shear-wave elastography (SWE) in assessing various musculoskeletal tissues, including tendons, muscles, nerves, and ligaments [53]. This technique is particularly noteworthy for its objectivity, quantifiable characteristics, and repeatability, making it an invaluable tool in determining the severity of musculoskeletal diseases and monitoring treatment outcomes. Their study also utilized ultrasound as the data acquisition method, which aligns with our own methodology. Therefore, the integration of AI models for anatomical segmentation could potentially complement elasticity imaging techniques, thereby reinforcing their clinical significance and paving the way for more comprehensive and personalized healthcare solutions.

Our exploration of the U-Net architecture revealed that its auto-crop functionality outperformed other models in isolating regions of interest. This automated feature is pivotal in enhancing the efficiency of image analysis, especially when dealing with vast datasets. Even though our elastography auto-crop pipeline testing encompassed only three subjects, the findings are indicative of its broader applicability and potential. In clinical scenarios, where time is of essence and precision is paramount, U-Net's auto-crop can streamline workflows. By automating the segmentation process, it ensures consistent and accurate isolation of regions across different scans and patients. As elasticity imaging techniques like SWE gain traction in the medical community, the integration of AI tools, such as U-Net's auto-crop, can further improve their accuracy and reliability. This leads to better patient care and more tailored treatment approaches.

D. CHALLENGES AND FUTURE DIRECTIONS

There are several clinical applications of this study. First, we proposed a method based on the anatomical standard plane and deep learning methods to segment various soft tissues of the shoulder. The use of standard planes is widely used in clinical practice of ultrasound on assessing fetus and internal organs [54]; however, the standard planes are

not used in musculoskeletal ultrasound [55]. The use of the anatomical standard plane can significantly reduce the need for a large dataset for the deep learning model. Our study is based on both the standard planes and deep learning methods and the results have demonstrated it is potential in establishing various deep learning models for the segmentation of muscles, subcutaneous tissues and bone. Second, although machine learning approaches have been used in musculoskeletal ultrasound, these studies focus on the segmentation of muscle tear within a muscle [6]. Our study explored the use of deep learning on the segmentation of various soft tissues. Third, our method can be used to segment soft tissues from elastographic ultrasound images. For elastographic ultrasound image analysis, a rectangular region of interest is usually selected to assess stiffness changes [33], [56]. Our method can facilitate the assessment of changes in specific soft tissues after rehabilitation and sports training [9]. Fourth, our method can also facilitate the assessment of soft tissues around a joint [57]. Although machine learning has demonstrated the potential on assessing muscle tear from a muscle, there remains many unsolved research problems such as using a machine learning approach to classify and segment multiple muscles consisting of vary distinct structural and biomechanical properties (eg. supraspinatus vs posterior deltoid of the shoulder joint), tendons and ligament at the same time. Our results further support the use of machine learning for the segmentation of mixed soft tissues. There remains a strong need for using machine learning approaches to improve clinical practice on using ultrasound to assess the effectiveness of rehabilitation interventions and sports training.

However, our study encountered several challenges that warrant attention for future work. The accurate recognition of tendons emerged as a particularly intricate task, even for seasoned human observers, underscoring the inherent complexities in shoulder muscle segmentation. This calls for the development of more refined labeling techniques or specialized models tailored for tendon recognition. We also noted boundary artifacts in our predicted images, a common issue in CNN-based segmentation models, which contrasted sharply with the more defined ground truth. The limited size of our dataset further exacerbated these challenges, falling short of the optimal requirements for robust model performance [58]. We aim to address these limitations in future research by exploring advanced labeling techniques and expanding our dataset.

V. CONCLUSION

Our research demonstrates the feasibility of using deep learning models of artificial intelligence in aiding clinicians to interpret the structures from shoulder ultrasound images. The results indicate that the U-Net model outperformed the Mask R-CNN and DeepLab V3+ models, exhibiting superior metrics in terms of mAP, Precision, Recall, and mIoU for the segmentation of soft tissue from the shoulder ultrasound images. This study provides the foundation to develop a robust and reliable tool to improve the classification and diagnosis of injured area from shoulder ultrasound images.

REFERENCES

[1] B. Tian, S. Yu, J. Chu, and W. Li, "Shoulder girdle muscle activity and fatigue during automobile chassis repair," *Int. J. Occupational Med. Environ. Health*, vol. 32, no. 4, pp. 537–552, 2019.
[2] J. Luime, B. Koes, I. Hendriksen, A. Burdorf, A. Verhagen, H. Miedema, and J. Verhaar, "Prevalence and incidence of shoulder pain in the general population; A systematic review," *Scandin. J. Rheumatol.*, vol. 33, no. 2, pp. 73–81, Mar. 2004.
[3] Y. Tang, Z. Chen, and X. Lin, "Characteristics and rehabilitation training effects of shoulder joint dysfunction in volleyball players under the background of artificial intelligence," *Comput. Intell. Neurosci.*, vol. 2022, pp. 1–12, Jun. 2022.
[4] H. Ramdev, "Shear wave ultrasound elastography of the shoulder joint tendons," M.S. thesis, Dept. Radiogr., Fac. Health Sci., Durban Univ., Durban, South Africa, 2020.
[5] J. A. Jacobson, "Shoulder U.S.: Anatomy, technique, and scanning pitfalls," *Radiology*, vol. 260, no. 1, pp. 6–16, Jul. 2011.
[6] L. Bonaldi, A. Pretto, C. Pirri, F. Uccheddu, C. G. Fontanella, and C. Stecco, "Deep learning-based medical images segmentation of musculoskeletal anatomical structures: A survey of bottlenecks and strategies," *Bioengineering*, vol. 10, no. 2, p. 137, Jan. 2023.
[7] J. Kemnitz, F. Eckstein, A. G. Culvenor, A. Ruhdorfer, T. Dannhauer, S. Ring-Dimitriou, A. M. Sänger, and W. Wirth, "Validation of an active shape model-based semi-automated segmentation algorithm for the analysis of thigh muscle and adipose tissue cross-sectional areas," *Magn. Reson. Mater. Phys., Biol. Med.*, vol. 30, no. 5, pp. 489–503, Oct. 2017.
[8] Z. Liu, J. Sun, M. Smith, L. Smith, and R. Warr, "Unsupervised subsegmentation for pigmented skin lesions," *Skin Res. Technol.*, vol. 18, no. 1, pp. 77–87, Feb. 2012.
[9] G. Lumsden, K. Lucas-Garner, S. Sutherland, and R. Dodenhoff, "Physiotherapists utilizing diagnostic ultrasound in shoulder clinics. How useful do patients find immediate feedback from the scan as part of the management of their problem?" *Musculoskeletal Care*, vol. 16, no. 1, pp. 209–213, Mar. 2018.
[10] J. A. Noble and D. Boukerroui, "Ultrasound image segmentation: A survey," *IEEE Trans. Med. Imag.*, vol. 25, no. 8, pp. 987–1010, Aug. 2006.
[11] U. Schneider, I. Graß, M. Laudien, J. Quetz, H. Graefe, B. Wollenberg, and J. E. Meyer, "Comparison of clinical examination and various imaging modalities in the diagnosis of head and neck cancer," *Int. Arch. Otorhinolaryngol.*, vol. 25, no. 2, pp. e179–e184, Apr. 2021.
[12] J. Zhao, W. Zheng, L. Zhang, and H. Tian, "Segmentation of ultrasound images of thyroid nodule for assisting fine needle aspiration cytology," *Health Inf. Sci. Syst.*, vol. 1, no. 1, pp. 1–12, Dec. 2013.
[13] J. Herrmann, G. Koerzdoerfer, D. Nickel, M. Mostapha, M. Nadar, S. Gassenmaier, T. Kuestner, and A. E. Othman, "Feasibility and implementation of a deep learning MR reconstruction for TSE sequences in musculoskeletal imaging," *Diagnostics*, vol. 11, no. 8, p. 1484, Aug. 2021.
[14] K. Tokuda, B. Lee, Y. Shiihara, K. Takahashi, N. Wada, K. Shirakura, and H. Watanabe, "Muscle activation patterns in acceleration-based phases during reach-to-grasp movement," *J. Phys. Therapy Sci.*, vol. 28, no. 11, pp. 3105–3111, 2016.
[15] M. E. Crommert, K. Halvorsen, and M. M. Ekblom, "Trunk muscle activation at the initiation and braking of bilateral shoulder flexion movements of different amplitudes," *PLoS ONE*, vol. 10, no. 11, Nov. 2015, Art. no. e0141777.
[16] R. P. Ottenheijm, M. J. Jansen, J. B. Staal, A. van den Bruel, R. E. Weijers, R. A. de Bie, and G.-J. Dinant, "Accuracy of diagnostic ultrasound in patients with suspected subacromial disorders: A systematic review and meta-analysis," *Arch. Phys. Med. Rehabil.*, vol. 91, no. 10, pp. 1616–1625, Oct. 2010.
[17] Y. Shin, J. Yang, Y. H. Lee, and S. Kim, "Artificial intelligence in musculoskeletal ultrasound imaging," *Ultrasonography*, vol. 40, no. 1, pp. 30–44, Jan. 2021.
[18] G. Litjens, T. Kooi, B. E. Bejnordi, A. A. A. Setio, F. Ciompi, M. Ghafoorian, J. A. Van Der Laak, B. van Ginneken, and C. I. Sánchez, "A survey on deep learning in medical image analysis," *Med. Image Anal.*, vol. 42, pp. 60–88, Dec. 2017.
[19] D. Shen, G. Wu, and H. I. Suk, "Deep learning in medical image analysis," *Annu. Rev. Biomed. Eng.*, vol. 19, pp. 221–248, Jun. 2017.

[20] J.-Y. Tsai, I. Y.-J. Hung, Y. L. Guo, Y.-K. Jan, C.-Y. Lin, T. T.-F. Shih, B.-B. Chen, and C.-W. Lung, "Lumbar disc herniation automatic detection in magnetic resonance imaging based on deep learning," *Frontiers Bioeng. Biotechnol.*, vol. 9, Aug. 2021, Art. no. 708137.
[21] F. Liao and Y.-K. Jan, "Assessing skin blood flow function in people with spinal cord injury using the time domain, time–frequency domain and deep learning approaches," *Biomed. Signal Process. Control*, vol. 84, Jul. 2023, Art. no. 104790.
[22] R. Brehar, D.-A. Mitrea, F. Vancea, T. Marita, S. Nedevschi, M. Lupsor-Platon, M. Rotaru, and R. I. Badea, "Comparison of deep-learning and conventional machine-learning methods for the automatic recognition of the hepatocellular carcinoma areas from ultrasound images," *Sensors*, vol. 20, no. 11, p. 3085, May 2020.
[23] O. Ronneberger, P. Fischer, and T. Brox, "U-Net: Convolutional networks for biomedical image segmentation," 2015, *arXiv:1505.04597*.
[24] K. He, G. Gkioxari, P. Dollár, and R. Girshick, "Mask R-CNN," 2017, *arXiv:1703.06870*.
[25] L.-C. Chen, Y. Zhu, G. Papandreou, F. Schroff, and H. Adam, "Encoder–decoder with atrous separable convolution for semantic image segmentation," 2018, *arXiv:1802.02611*.
[26] C. Shorten and T. M. Khoshgoftaar, "A survey on image data augmentation for deep learning," *J. Big Data*, vol. 6, no. 1, pp. 1–48, Dec. 2019.
[27] A. Goyal, A. Razik, D. Kandasamy, A. Seth, P. Das, B. Ganeshan, and R. Sharma, "Role of MR texture analysis in histological subtyping and grading of renal cell carcinoma: A preliminary study," *Abdominal Radiol.*, vol. 44, no. 10, pp. 3336–3349, Oct. 2019.
[28] M. van Holsbeeck, S. Soliman, F. Van Kerkhove, and J. Craig, "Advanced musculoskeletal ultrasound techniques: What are the applications?" *Amer. J. Roentgenol.*, vol. 216, no. 2, pp. 436–445, Feb. 2021.
[29] P. Ardhianto, J.-Y. Tsai, C.-Y. Lin, B.-Y. Liau, Y.-K. Jan, V. B. H. Akbari, and C.-W. Lung, "A review of the challenges in deep learning for skeletal and smooth muscle ultrasound images," *Appl. Sci.*, vol. 11, no. 9, p. 4021, Apr. 2021.
[30] Y. Li, P.-C. Mo, S. Jain, J. Elliott, A. Bleakney, S. Lyu, and Y.-K. Jan, "Effect of durations and pressures of cupping therapy on muscle stiffness of triceps," *Frontiers Bioeng. Biotechnol.*, vol. 10, Nov. 2022, Art. no. 996589.
[31] G. Cocco, V. Ricci, A. Boccatonda, G. Iannetti, and C. Schiavone, "Migration of calcium deposit over the biceps brachii muscle, a rare complication of calcific tendinopathy: Ultrasound image and treatment," *J. Ultrasound*, vol. 21, no. 4, pp. 351–354, Dec. 2018.
[32] J. H. Oh, J. Y. Kim, D. H. Kim, Y. I. Kim, and J. H. Cho, "Sonoelastography on supraspinatus muscle-tendon and long head of biceps tendon in Korean professional baseball pitchers," *Korean J. Sports Med.*, vol. 34, no. 1, p. 28, 2016.
[33] Y.-K. Jan, X. Hou, X. He, C. Guo, S. Jain, and A. Bleakney, "Using elastographic ultrasound to assess the effect of cupping size of cupping therapy on stiffness of triceps muscle," *Amer. J. Phys. Med. Rehabil.*, vol. 100, no. 7, pp. 694–699, Jul. 2021.
[34] B. C. Russell, A. Torralba, K. P. Murphy, and W. T. Freeman, "LabelMe: A database and web-based tool for image annotation," *Int. J. Comput. Vis.*, vol. 77, nos. 1–3, pp. 157–173, May 2008.
[35] F. Ponti, A. De Cinque, N. Fazio, A. Napoli, G. Guglielmi, and A. Bazzocchi, "Ultrasound imaging, a stethoscope for body composition assessment," *Quant. Imag. Med. Surgery*, vol. 10, no. 8, pp. 1699–1722, Aug. 2020.
[36] S. Saha and M. Baumert, "Intra- and inter-subject variability in EEG-based sensorimotor brain computer interface: A review," *Frontiers Comput. Neurosci.*, vol. 13, p. 87, Jan. 2020.
[37] Q. H. Nguyen, H.-B. Ly, L. S. Ho, N. Al-Ansari, H. V. Le, V. Q. Tran, I. Prakash, and B. T. Pham, "Influence of data splitting on performance of machine learning models in prediction of shear strength of soil," *Math. Problems Eng.*, vol. 2021, pp. 1–15, Feb. 2021.
[38] G. An, M. Akiba, K. Omodaka, T. Nakazawa, and H. Yokota, "Hierarchical deep learning models using transfer learning for disease detection and classification based on small number of medical images," *Sci. Rep.*, vol. 11, no. 1, p. 4250, Mar. 2021.
[39] M. Mubashar, H. Ali, C. Gronlund, and S. Azmat, "R2U++: A multiscale recurrent residual U-Net with dense skip connections for medical image segmentation," 2022, *arXiv:2206.01793*.
[40] C. Lu, Z. Fu, Z. Fu, and J. Fei, "Prior region mask R-CNN for thyroid nodule segmentation in ultrasound images," in *Proc. Int. Conf. Intell. Robot. Appl.* Cham, Switzerland: Springer, 2023, pp. 105–116.
[41] R. Azad, M. Heidari, M. Shariatnia, E. K. Aghdam, S. Karimijafarbigloo, E. Adeli, and D. Merhof, "TransDeepLab: Convolution-free transformer-based DeepLab V3+ for medical image segmentation," in *Proc. Int. Workshop Predictive Intell. Med.* Switzerland: Springer, 2022, pp. 91–102.
[42] L. Perez and J. Wang, "The effectiveness of data augmentation in image classification using deep learning," 2017, *arXiv:1712.04621*.
[43] Bubbliiiing. (2022). *UNet-TF2*. [Online]. Available: https://github.com/bubbliiiing/unet-tf2
[44] Bubbliiiing. (2022). *DeepLabV3-Plus-Tf2*. [Online]. Available: https://github.com/bubbliiiing/deeplabv3-plus-tf2
[45] Zouyuelin. (2022). *MASK_RCNN_2.5.0*. [Online]. Available: https://github.com/zouyuelin/MASK_RCNN_2.5.0
[46] Y. Bengio, A. Courville, and P. Vincent, "Representation learning: A review and new perspectives," *IEEE Trans. Pattern Anal. Mach. Intell.*, vol. 35, no. 8, pp. 1798–1828, Aug. 2013.
[47] R. D. Peng, "Reproducible research in computational science," *Science*, vol. 334, no. 6060, pp. 1226–1227, Dec. 2011.
[48] K. Lee, J. Y. Kim, M. H. Lee, C.-H. Choi, and J. Y. Hwang, "Imbalanced loss-integrated deep-learning-based ultrasound image analysis for diagnosis of rotator-cuff tear," *Sensors*, vol. 21, no. 6, p. 2214, Mar. 2021.
[49] Y.-W. Wang, C.-C. Lee, and C.-M. Lo, "Supraspinatus segmentation from shoulder ultrasound images using a multilayer self-shrinking snake," *IEEE Access*, vol. 7, pp. 146724–146731, 2019.
[50] H. Kim, K. Shin, H. Kim, E.-S. Lee, S. W. Chung, K. H. Koh, and N. Kim, "Can deep learning reduce the time and effort required for manual segmentation in 3D reconstruction of MRI in rotator cuff tears?" *PLoS ONE*, vol. 17, no. 10, Oct. 2022, Art. no. e0274075.
[51] K. J. Edmunds, M. K. Gíslason, I. D. Arnadottir, A. Marcante, F. Piccione, and P. Gargiulo, "Quantitative computed tomography and image analysis for advanced muscle assessment," *Eur. J. Transl. Myol.*, vol. 26, no. 2, p. 6015, Jun. 2016.
[52] H. Guo, G. He, W. Jiang, R. Yin, L. Yan, and W. Leng, "A multi-scale water extraction convolutional neural network (MWEN) method for GaoFen-1 remote sensing images," *ISPRS Int. J. Geo-Inf.*, vol. 9, no. 4, p. 189, Mar. 2020.
[53] M. S. Taljanovic, L. H. Gimber, G. W. Becker, L. D. Latt, A. S. Klauser, D. M. Melville, L. Gao, and R. S. Witte, "Shear-wave elastography: Basic physics and musculoskeletal applications," *RadioGraphics*, vol. 37, no. 3, pp. 855–870, May 2017.
[54] H. Chen, L. Wu, Q. Dou, J. Qin, S. Li, J.-Z. Cheng, D. Ni, and P.-A. Heng, "Ultrasound standard plane detection using a composite neural network framework," *IEEE Trans. Cybern.*, vol. 47, no. 6, pp. 1576–1586, Jun. 2017.
[55] R. Tang, Z. Li, L. Jiang, J. Jiang, B. Zhao, L. Cui, G. Zhou, X. Chen, and D. Jiang, "Development and clinical application of artificial intelligence assistant system for rotator cuff ultrasound scanning," *Ultrasound Med. Biol.*, vol. 50, no. 2, pp. 251–257, Feb. 2024.
[56] I. Y.-J. Hung and Y.-K. Jan, "Using texture analysis of ultrasound images to assess the effect of cupping therapy on muscle quality of the triceps," *PLoS ONE*, vol. 19, no. 3, Mar. 2024, Art. no. e0301221.
[57] S. Salehi, A. Shadmehr, G. Olyaei, S. Bashardoust, and S. M. Mir, "Effects of dry needling and stretching exercise versus stretching exercise only on pain intensity, function, and sonographic characteristics of plantar fascia in the subjects with plantar fasciitis: A parallel single-blinded randomized controlled trial," *Physiotherapy Theory Pract.*, vol. 39, no. 3, pp. 490–503, Mar. 2023.
[58] M. H. Hesamian, W. Jia, X. He, and P. Kennedy, "Deep learning techniques for medical image segmentation: Achievements and challenges," *J. Digit. Imag.*, vol. 32, no. 4, pp. 582–596, Aug. 2019.

YING-CHUN LEE is currently pursuing the Senior Electrical Engineering with Yuan Ze University, Taiwan, specializing in AI programming. He has a deep interest in the field of robotics and has proven his prowess by securing first place in a combat robot competition during his university years. From a young age, he has been fascinated with programming and has mastered languages, such as C++ and Python. Currently, he is researching medical AI image models with an aspiration to contribute to the healthcare field. His dedication to technology and healthcare, combined with his development fields, aiming to innovate and make significant contributions to the world of programming.

CHIH-YANG LIN (Senior Member, IEEE) is currently with the Department of Mechanical Engineering, National Central University, Taoyuan, Taiwan. He has been recognized as an IET fellow and has contributed more than 150 papers that have been featured in a wide range of international conferences and journals. His research interests include computer vision, machine learning, deep learning, image processing, big data analysis, and the design of surveillance systems.

CHIA-CHUN HSIAO received the bachelor's degree in electrical and communication engineering from Yuan Ze University, Taiwan, in 2022. Her current research interests include image processing and computer vision applications with deep learning.

PU-CHUN MO was born in Kaohsiung City, Taiwan, in 1991. He received the B.S. and M.S. degrees in occupational therapy from National Cheng Kung University, in 2015, where he is currently pursuing the Ph.D. degree in biomedical engineering, under Prof. Fong-Chin Su. He was a Research Assistant with the Rehabilitation Technology and Biomechanics Laboratory, from 2013 to 2015, with Prof. Li-Chieh Kuo. From 2015 to 2017, he was a Research Assistant with the Human Dynamics Laboratory. From 2017 to 2019, he was with the Medical Device Innovation Center as an Engineering Group Leader in developing a long-term care AI system. He was affiliated with the University of Illinois at Urbana-Champaign. He is the author of seven articles. His research interests include human motion movement, rehabilitation science, medical device development, and AI application in medical fields. He was in the top five conference papers in the International Society of Biomechanics, in 2017.

JIAQI GUO received the Bachelor of Science degree from the University of Illinois at Urbana–Champaign, in 2023, USA, where he is currently pursuing the Ph.D. degree in kinesiology. In his role as a Research Assistant with the Rehabilitation Engineering Laboratory, he is committed to advancing knowledge in kinesiology. He is a dedicated Researcher in the field of kinesiology, specializing in biomechanics. His research interests center around investigating the biomechanical properties of soft tissues in individuals with disabilities.

YIH-KUEN JAN is currently the Director and an Associate Professor with the Rehabilitation Engineering Research Laboratory, University of Illinois at Urbana–Champaign (UIUC). He is committed to developing rehabilitation technologies for the prevention and management of secondary conditions in people with impaired mobility. He is recognized for his research on soft tissue biomechanics and its role in the development of musculoskeletal injuries and pressure injuries. He has extensively published his research work to improve the understanding of the effect of various pathophysiological conditions (spinal cord injury, aging, diabetes, and physical inactivity) on musculoskeletal injury.